Molecular Vision 2017; 23:680-694 <http://www.molvis.org/molvis/v23/680>
Received 10 April 2017 | Accepted 1 October 2017 | Published 3 October 2017

© 2017 Molecular Vision

Multicellular tumor spheroids of human uveal melanoma induce genes associated with anoikis resistance, lipogenesis, and SSXs

Charlotte Ness,[1,2] Øystein Garred,[3] Nils A. Eide,[1] Theresa Kumar,[3] Ole K. Olstad,[4] Thomas P. Bærland,[1] Goran Petrovski,[1,2] Morten C. Moe,[1,2] Agate Noer[1,2]

(The last two authors co-senior authors for this study)

[1]Center for Eye Research, Department of Ophthalmology, Oslo University Hospital and University of Oslo, Norway; [2]Norwegian Center for Stem Cell Research, Oslo University Hospital, Norway; [3]Department of Pathology, Oslo University Hospital, Norway; [4]Department of Medical Biochemistry, Oslo University Hospital, Norway

Purpose: Uveal melanoma (UM) has a high propensity for metastatic spread, and approximately 40–50% of patients die of metastatic disease. Metastases can be found at the time of diagnosis but also several years after the primary tumor has been removed. The survival of disseminated cancer cells is known to be linked to anchorage independence, anoikis resistance, and an adaptive cellular metabolism. The cultivation of cancer cells as multicellular tumor spheroids (MCTS) by anchorage-independent growth enriches for a more aggressive phenotype. The present study examines the differential gene expression of adherent cell cultures, non-adherent MCTS cultures, and uncultured tumor biopsies from three patients with UM. We elucidate the biochemical differences between the culture conditions to find whether the culture of UM as non-adherent MCTS could be linked to an anchorage-independent and more aggressive phenotype, thus unravelling potential targets for treatment of UM dissemination.

Methods: The various culture conditions were evaluated with microarray analysis, quantitative reverse-transcription polymerase chain reaction (qRT-PCR), RNAscope, immunohistochemistry (IHC), and transmission electron microscopy (TEM) followed by gene expression bioinformatics.

Results: The MCTS cultures displayed traits associated with anoikis resistance demonstrated by *ANGPTL4* upregulation, and a shift toward a lipogenic profile by upregulation of *ACOT1* (lipid metabolism), *FADS1* (biosynthesis of unsaturated fatty acids), *SC4MOL*, *DHCR7*, *LSS* (cholesterol biosynthesis), *OSBPL9* (intracellular lipid receptor), and *PLIN2* (lipid storage). Additionally, the present study shows marked upregulation of synovial sarcoma X breakpoint proteins (SSXs), transcriptional repressors related to the Polycomb group (PcG) proteins that modulate epigenetic silencing of genes.

Conclusions: The MCTS cultures displayed traits associated with anoikis resistance, a metabolic shift toward a lipogenic profile, and upregulation of SSXs, related to the PcG proteins.

Uveal melanoma (UM) is the most common primary intraocular malignancy in adults with an incidence of approximately 5.1 per million per year in the United States [1], while in Europe, the incidence varies from less than 2 per million per year in Spain and southern Italy to more than 8 per million per year in Scandinavia [2,3]. Despite advances in the diagnosis and treatment of the disease, the prognosis has remained largely unchanged [1,4]. UM has a high propensity for metastatic spread. Relapse can be seen several years after treatment, and 40–50% of patients will eventually die of metastatic disease [4-7]. Dissemination of cancer cells from the primary tumor is believed to be an early event in UM. Circulating malignant cells (CMCs) have been detected in up to 88% of patients with UM and can be found at the time of diagnosis but also years after the primary tumor has been removed [8]. Micrometastatic cells have also been found in the bone marrow of patients with UM in 29% of cases [9]. Intriguingly, the presence of disseminated cells in bone marrow and the bloodstream does not correlate with overall survival [8,10]. Cancer cells disseminating from the primary tumor have to adapt to a changing micromilieu to generate metastatic disease. The various tissues of the metastatic route provide a different nutritional supply, pH, and oxygen concentration; thus, the malignant cells have to exhibit metabolic flexibility to sustain growth and survival [11-13].

Anchorage-independent growth and resistance to anoikis (cell death induced by loss of extracellular matrix attachment as in circulating metastatic cells) are essential features of disseminated cancer cells and metastatic progression [14-16]. The generation of multicellular tumor spheroids (MCTS) by anchorage-independent growth is associated with enrichment of an aggressive phenotype characterized by chemoresistance, invasiveness, and expression of undifferentiated markers [17-21]. The present study aims to compare the differential

Correspondence to: Agate Noer, Center for Eye Research, Department of Ophthalmology, Oslo University Hospital, Postboks 4956 Nydalen 0424 Oslo, Norway; Phone: +47 23 01 61 98; FAX: +47 22 11 80 00; email: agate.noer@medisin.uio.no

gene expression of MCTS of UM to primary tumor tissue and adherent cultures, with a special emphasis on unravelling the pathways and survival mechanisms pathognomonic for disseminated and circulating cancer cells.

METHODS

All experiments were conducted in accordance with the Declaration of Helsinki (2013), and all tissue harvesting was approved by the Local Committees for Medical Research Ethics (REK Ref. 2009/1973 and REK Ref. 2013/803–1). The study is adhered to the ARVO statement on human subjects. Informed written consent was obtained from patients before tissue harvesting. All reagents used in the present study were from Sigma-Aldrich (St. Louis, MO) unless otherwise stated.

Biopsies and cell cultures: UM biopsies from patients undergoing enucleation of the eye were included in this study. After enucleation, the ophthalmic pathologist excised fresh tumor tissue for use in research before formalin fixation for routine histopathological examination. The UM of the three donors (D1, D2, and D3) was classified as mixed (D1) and epithelioid (D2 and D3) types with a routine histopathological examination. Retrospectively, donors D1, D2, and D3 all had confirmed liver metastases. A fourth supplementary donor was added to the study after data were obtained. The UM of this donor, D(S), was classified as epithelioid, and the donor tissue underwent the same culture conditions as the tissue from donors D1, D2, and D3.

A fraction of the tissue was snap-frozen and stored at −80 °C. The remaining sample was minced with scissors in collagenase I and IV (1 mg/ml), before being incubated for 1 h at 37 °C. After dissociation, the tissue was cultured adherently for 7 days in RPMI 1640 (Invitrogen, Carlsbad, CA), 10% fetal bovine serum (FBS), penicillin/streptomycin (100 U/ml, P4333), and amphotericin B (2.5 µg/ml, A2942) in addition to gentamycin (75 µg/ml; Sanofi-Aventis, Gentilly, France) to ensure the removal of fibroblasts [22]. After 7 days of adherent culturing, the cells were trypsinized using Trypsin-EDTA (0.25%, T4049) and pelleted into three fractions of 100,000 cells. The first fraction of the cells was collected for RNA analyses, the second fraction for further adherent growth, and the third for non-adherent growth as MCTS. The term MCTS is used for this non-adherent culture of tumor cells, in accordance with the nomenclature, and is considered aggregation and compaction of tumor cells [21]. The cell fraction for MCTS culture was plated at a density of 500–1,000 cells per well on Corning Costar ultra-low attachment, polystyrene, round-bottom 96-well plates (CLS7007) in melanoma stem cell medium (MSCM) (1) and (2): (1) 30% human embryonic stem cell medium (hESC); (78% KnockOut DMEM/F12 (Cat. no. 12660–012, Thermo Fisher Scientific Inc., Waltham, MA), 20% KnockOut serum replacer (Cat. no. 10828–028, Thermo Fisher Scientific Inc.), 1% MEM non-essential amino acids (Cat. no. 11140–050, Thermo Fisher Scientific Inc.), 4 ng/ml basic fibroblast growth factor (b-FGF; Cat. no. 13,256-029, Thermo Fisher Scientific Inc.), 1% GlutaMAX (35,050-061, Thermo Fisher Scientific Inc.), and 1.4‰ 2-mercaptoethanol (M7522) and (2) 70% mouse embryonic fibroblast (MEF) conditioned medium (AR005, R&D Systems/Bio-Techne, Minneapolis, MN) [23] with penicillin/streptomycin (100 U/ml) and amphotericin B (2.5 µg/ml). The cells were collected after 12 days of cell culture and further embedded in paraffin for immunohistochemistry (IHC) or pelleted and stored at −80 °C for RNA analyses.

RNA isolation: RNA from fresh frozen primary tumors (D1, D2, and D3) was isolated using the Qiagen RNeasy kit (Qiagen, Hilden, Germany). Briefly, the tissue was placed in a 4.5 ml cryotube, and 500 µl of QIAzol (Qiagen) was added before the sample was disrupted using Qiagen TissueRuptor (Qiagen), according to the manufacturer's recommendations. The sample was centrifuged at 18 400 ×g for 10 min to remove insoluble material before being processed with the Qiagen RNeasy kit with DNase. Samples were purified using the Zymo PCR inhibitor removal kit (Zymo, Irvine, CA). RNA from the pelleted samples (adherent and cultured spheres from D1, D2, and D3) was isolated as described above, except the disruption step using the Qiagen TissueRuptor. RNA concentration and purity were determined using NanoDrop (Wilmington, DE) and Bioanalyzer (Agilent 2100, Agilent, Santa Clara, CA). All nine samples had RNA integrity number (RIN) values above 8 before being analyzed with microarray and PCR [24].

Immunohistochemistry: The growth media in the 96-well plates was diluted by gently adding Hanks' Balanced Salt solution (Thermo Fisher Scientific Inc.). Then the MCTS were allowed to make sediment before the media was carefully removed. A mixture of human plasma and thrombin (Sigma–Aldrich) was used to clot the MCTS together before fixation in 4% paraformaldehyde (PFA) and embedment in paraffin. Then 3.5 µm sections were cut and stained [25]. K_i-67 staining was performed using the Envision + Dual Link HRP (K4065, Dako, Glostrup, Denmark) and AEC + Substrate chromogen ready-to-use (k3461, Dako). Briefly, the K4065 kit protocol was followed until the addition of 3,3′-diaminobenzidine (DAB). After polymer horseradish peroxidase (HRP), 3-amino-9-ethylcarbazole (AEC) chromogen from the kit k3461 was added, and the sections were washed and counterstained with hematoxylin according to the k3461 protocol. Negative controls without primary antibody

were included for all stainings. The following primary antibodies and dilutions were used (rabbit:rb, mouse:ms): K_i-67 (rb, 1:200; Thermo Fisher Scientific Inc.), SSX4 (rb, 1;50; Acris), anti-melanoma (a-melanoma) [HMB45 + MART1 (DT101 + BC199) + tyrosinase (T311)] (ms, 1:50; ab733, Abcam, Cambridge, UK), Perilipin (rb, 1:100; Santa Cruz Biotechnology Inc., Dallas, TX), and ANGPTL4 (rb, 1:500; Abcam). The secondary antibodies had the fluorescent marker Alexa Fluor 488 (1:500; Invitrogen). Hoechst (1:500; Invitrogen) was used for nuclear staining. The sections were analyzed using a Zeiss Axio Observer.Z1 fluorescence microscope (Zeiss, Oberkochen, Germany). Sections were also stained with hematoxylin and eosin (H&E) for morphological examination.

Microarray: Microarray analysis was performed at the Genomics Core Facility, Oslo University Hospital and Helse Sør-Øst. HumanHT-12 v4 Expression BeadChip (Illumina, San Diego, CA) was used for the analysis. It targets more than 31,000 annotated genes with 47,000 probes mainly derived from the National Center for Biotechnology Information Reference Sequence (NCBI) RefSeq Release 38 (November 7, 2009). For each sample, 440 ng of total RNA was amplified and labeled using the Illumina TotalPrep-96 RNA Amplification Kit protocol. The quantity of labeled copy RNA (cRNA) was measured using the NanoDrop spectrophotometer (Wilmington, DE). The quality and size distribution of the labeled cRNA were assessed using the 2100 Bioanalyzer. This was done to be able to hybridize equal amounts of successfully labeled cRNA to the arrays. For each sample, 750 ng of biotin-labeled cRNA was hybridized to the Illumina HumanHT-12 v4 Expression BeadChip. J-Express and rank product (RP) analysis were used to further identify differently expressed genes with ≥2 fold up- or downregulation and q values ≤0.05 between the different groups. One thousand permutations (1,000*) were run for each RP analysis [26].

Quantitative reverse-transcription PCR: RNA concentration and purity were measured using NanoDrop. Reverse transcription (RT) was performed using the High Capacity cDNA Reverse Transcription Kit (Applied Biosystems, Abingdon, UK) with 50 ng total RNA per 20 µl RT reaction. Copy DNA (cDNA) was diluted to a volume of 50 µl (1 ng/µl) after cDNA synthesis. Quantitative PCR (qPCR) was performed using the StepOnePlus RT–PCR system (Applied Biosystems) and Taqman Gene Expression assays following the manufacturer's protocols (Applied Biosystems). The TaqMan Gene Expression Assays used include *ANGPTL4* (Hs01101127_m1) and *18S* (Hs03003631_g1). The thermal cycling conditions were 95 °C for 10 min followed by 40 cycles of 95 °C for 15 s and 60 °C for 1 min. All samples were run in duplicate (each reaction: 2.5 µl/2.5 ng cDNA in a total volume of 12.5 µl). The data were analyzed using the $2^{-\Delta\Delta Ct}$ method to find the relative changes in gene expression as a fold change between the samples. The uncultured tumor sample was chosen as the calibrator and equaled one, while the other samples had fold changes related to the uncultured tumor calibrator sample. The 18S probe, primers, and assay (Hs03003631_g1) were used as a loading control to quantify the differences in cDNA input between the samples.

RNAscope in situ hybridization: RNA in situ hybridization was performed using the RNAscope® 2.5 High Definition (HD)- Red assay (Advanced Cell Diagnostics, Hayward, CA) according to the manufacturer's instructions using the standard pretreatment protocol. Sections were mounted using Prolong Gold with 4',6-diamidine-2'-phenylindole dihydrochloride (DAPI). RNAscope permits direct visualization of RNA in formalin-fixed, paraffin-embedded (FFPE) tissue with single molecule sensitivity and single cell resolution [27]. RNAscope Probe-Hs-SSX4–01 (Cat. no. 468,641, Advanced Cell Diagnostics) was used. Hybridization signals were detected with chromogenic reactions using Fast Red. Fast Red produces red fluorescence in addition to the red reaction product, thus providing a greater level of sensitivity [28]. The RNA staining signal was identified as red punctate dots. Each sample was quality controlled for RNA integrity with a probe specific to peptidyl-prolyl cis-trans isomerase B (PPIB) mRNA. Negative control background staining was evaluated using a probe (Cat.no. 3100439, Advanced Cell Diagnostics, Newark, NJ) specific to the bacterial *dihydrodipicolinate reductase* (*DapB*) gene (Gene ID EF191515). The sections were analyzed with a Zeiss Axio Observer.Z1 fluorescence microscope.

Pathway and gene ontology analysis: Data from the microarray analysis were imported into Ingenuity Pathway Analysis (IPA) software in the search for biologic pathways and Gene Ontology to identify potential networks. Principal component analysis (PCA) and unsupervised hierarchical clustering were performed using the Partek Genomics Suite software (Partek, Inc., Chesterfield, MO).

Transmission electron microscopy: Primary tissue from uncultured tumor D1 and the donor D(S) cultured as MCTS were fixed at 4 °C overnight in glutaraldehyde (0.1 M). The tissue was washed four times in cacodylate buffer (0.2 M) before post-fixation in a mixture of 1% osmium tetroxide and cacodylate buffer (0.2 M) for 60 min. The tissue was further rinsed in cacodylate buffer (0.2 M) before being dehydrated through a graded series of ethanol up to 100%. The tissue was then immersed in propylene oxide for 2 ×5 min and a mixture of Epon and propylene oxide before embedment in

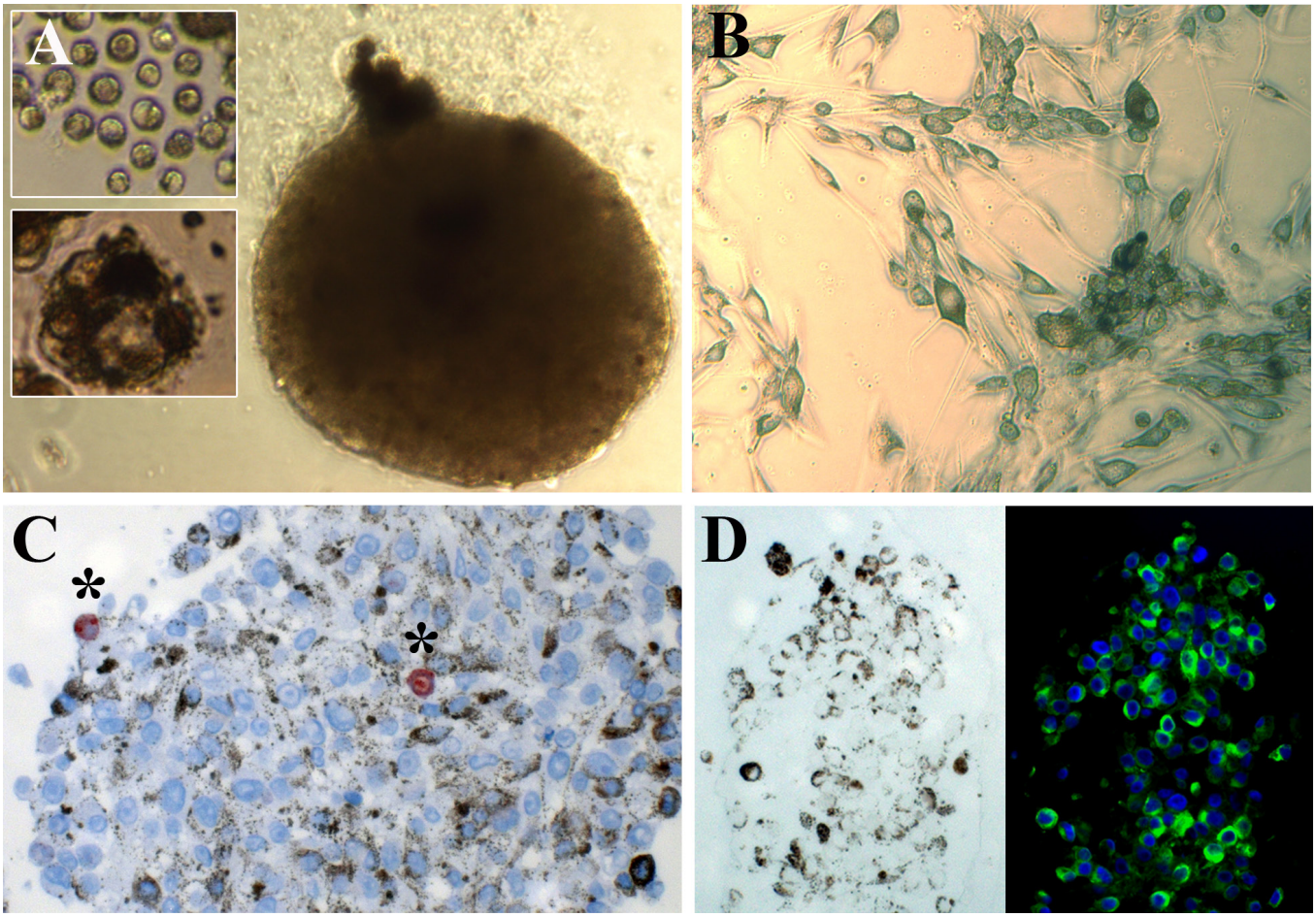

Figure 1. Multicellular tumor spheroid culture of primary uveal melanoma cells. **A**: Single cells (upper inset) after primary tumor isolation, during cultivation small pigmented tumor spheres formed (lower inset), and further developing resulting into large spheroid structures if not passaged. **B**: Adherent cell culture of primary uveal melanoma (UM) cells. **C**: Ki67 staining (*) of UM multicellular tumor spheroid (MCTS). **D**: Immunohistochemical staining of antimelanoma (green) and Hoechst staining of the nucleus (blue; right panel) with the corresponding light-microscopic image (left panel) of UM MCTS.

Epon. Ultrathin sections (60–70 nm thick) were cut on a Leica Ultracut Ultramicrotome UCT (Leica, Wetzlar, Germany), stained with uranyl acetate and lead citrate, and examined using a Tecnai12 transmission electron microscope (Phillips, Amsterdam, the Netherlands).

RESULTS

Cultivation of uveal melanoma: The cells cultured as MCTS grew as large aggregations involving the majority of the cells in the well (Figure 1A and insets). The MCTS were mitotically active, as seen with the positive Ki67 staining with a score of 1%, 2%, and 4% for donors D1, D2, and D3, respectively (Figure 1C). The melanoma profile of the MCTS was verified by staining for a-melanoma, a marker that recognizes HMB-45, MART-1, and tyrosinase. More than 90% of the cells in the MCTS-derived paraffin sections stained positive for this marker (Figure 1D).

Genetic clustering is determined by the culture conditions: The gene expression profiles of the UMs (D1, D2, and D3), uncultured, cultured as MCTS, or cultured as adherent primary cells, were comprehensively analyzed with microarray analysis. PCA was performed on raw data from the microarray with a false discovery rate (FDR) of 10%. This type of analysis clusters the samples and represents them on a three-dimensional space based on the differential relative gene expression. The PCA plot shows that the clustering was mainly determined by the culture conditions (Figure 2A).

The relative gene expression of UMs (uncultured, cultured as MCTS, or cultured as adherent primary tumor cells) was further investigated by performing an unsupervised

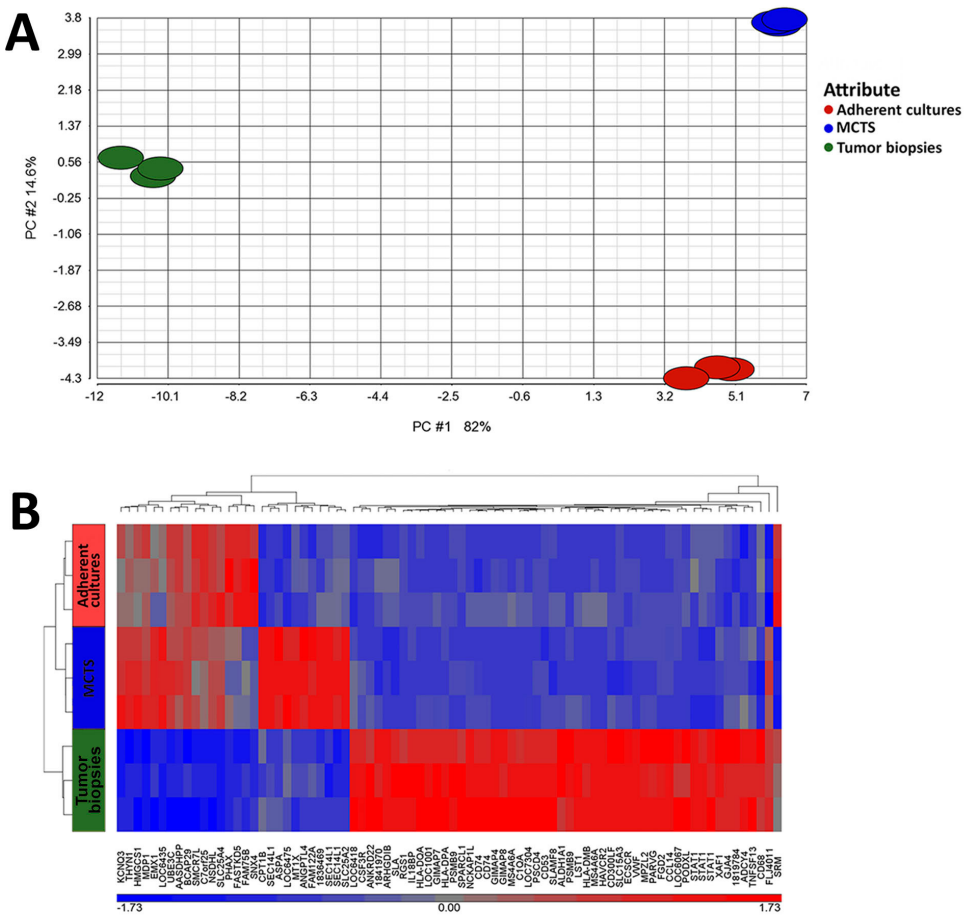

Figure 2. Gene expression in uveal melanoma donors (D1, D2, and D3) cultured as primary adherent cells (red), multicellular tumor spheroids (blue), and uncultured tumor biopsies (green). **A**: Principal component analysis (PCA) plot of gene expression in uveal melanoma donors (D1, D2, and D3) cultured as primary adherent cells (red), multicellular tumor spheroids (blue), and uncultured tumor biopsies (green). **B**: Hierarchical clustering of gene expression in uveal melanoma donors (D1, D2, and D3), where each row represents the single sample tested: adherent cultures (D1, D2, and D3; red), multicellular tumor spheroids (MCTS; D1, D2, and D3; blue), and uncultured tumors (D1, D2, and D3; green), while each column represents a single probe set (gene symbol or Illumina ID number) analyzed. Relative gene expression is presented in color: Red is higher-level expression relative to the sample mean, blue is relatively lower level expression, and gray is no change in expression.

hierarchical clustering with an FDR of 10% presented as a heat map (Figure 2B). The heat map shows significant downregulation of the surface markers in the cultured cells compared to the uncultured primary tumor biopsy. These markers reflect the cellular heterogeneity of the primary tumor and the loss of macrophages (CD68), endothelial cells (von Willebrand factor), and T-cells (CD3D, CD8A, and CD2) in the cell cultures (Table 1). Additionally, there is a marked downregulation of human leukocyte antigen (HLA) expression in MCTS (Table 1) and in the adherent primary tumor cells (Appendix 1). This finding is in accordance with the work of van Essen et al. who showed downregulation of HLA expression upon loss of tumor-infiltrating leukocytes [29].

The genes found to be upregulated in the unsupervised hierarchical clustering (Figure 2B) were in concordance with many of the genes found in the RP analysis (Table 1 and supplementary data). The RP analysis ($q \leq 0.05$) resulted in 206 genes ≥2 fold upregulated and 373 genes ≥2 fold downregulated in MCTS versus uncultured tumor biopsies. Two hundred eighteen genes were found to be ≥2 fold upregulated, and 552 genes were ≥2 fold downregulated in adherent cell cultures versus the uncultured tumor biopsies. Sixty-four genes were found to be ≥2 fold upregulated, and 71 genes were ≥2 fold downregulated in adherent cell cultures versus the MCTS.

The genes from the RP analysis were further analyzed with Ingenuity IPA software. The differences in molecular and cellular functions between the various culture conditions are shown in Figure 3.

There was a noticeable increase in the cellular strain in the MCTS compared to the uncultured tumor biopsies, indicated by increased free radical scavenging, enhanced drug metabolism, and the increase in lipid metabolism in the MCTS versus adherent cells and uncultured tumor biopsies. Associated pathways and molecules in lipid metabolism in the MCTS versus uncultured tumor biopsies are shown in Figure 3. Alterations in the lipid metabolism include seven networks:

synthesis of lipids, steroid metabolism, metabolism of cholesterol, metabolism of lipid membrane derivatives, synthesis of cholesterol, and conversion of lipid and fatty acid metabolism.

MCTS display a genetic profile indicating EMT and anoikis resistance: Anoikis is a form of apoptosis induced by loss or inappropriate cell adhesion [30]. The process of epithelial-to-mesenchymal-transition (EMT) is considered an important feature of anoikis [31]. Rank product data revealed 3.5-fold upregulation of *snail family transcriptional repressor 2* (*SNAI2;* Gene ID: 6591, OMIM 602150) and 0.6-fold downregulation of *cadherin 1* (*CDH1*; Gene ID: 999, OMIM 192090; E-cadherin) in MCTS (Table 1). Anoikis resistance is also supported by the upregulation of *pyruvate dehydrogenase kinase 4* (*PDK4;* Gene ID: 5166, OMIM 602527), an enzyme that inactivates pyruvate dehydrogenase (PDH), which is required for the conversion of pyruvate to acetyl-CoA. *PDK4* is upregulated in response to loss of adherence (LOA) and reduces reactive oxygen species (ROS) strain [32]. Noticeably, there was strong upregulation of *angiopoietin like 4* (*ANGPTL4;* Gene ID: 51129, OMIM 605910) in the MCTS (Table 1, Figure 4). *ANGPTL4* has recently been shown to be associated with an angiogenic phenotype of UM, and thus being involved in metastatic spread [33]. *ANGPTL4* is thought to contribute to anoikis resistance by inducing conformational changes that enable resistance to inducers of apoptosis [34,35]. *ANGPTL4* is further known to stimulate

Table 1. List of selected genes, including the ten most up- and downregulated, from the microarray rank product (RP) analysis (≥ 2fold up- or down- regulated, q≤0.05) in multicellular tumour spheroids (MCTS) versus uncultured tumours and MCTS versus adherent cultures (see supplementary data for the complete list).

Up in MCTS vs. uncultured tumours		Down in MCTS vs. uncultured tumours		Up in MCTS vs. adherent cultures		Down in MCTS vs. adherent cultures	
Gene symbol	**Fold change**	**Gene symbol**	**Fold change**	**Gene symbol**	**Fold change**	**Gene symbol**	**Fold change**
ANGPTL4	27.1	HLA-DRA	-32.1	ANGPTL4	21.1	VGF	-11
SSX4	6.4	CD74	-22.9	SSX4	6.2	ID3	-10.7
ASPA	4.7	C1QB	-17.8	ASPA	4.6	MIR1974	-5.9
SSX2	4.5	VWF	-14	SSX2	4.3	ILMN_1881909	-3.9
LDLR	4.4	CD14	-12.2	APOD	3.6	ID2	-4.6
MT1X	4.3	C1QC	-11.7	IL17D	3.2	CTGF	-4.1
HTR2B	4.3	HLA-DMB	-11.1	NRXN2	3.2	ID1	-3.9
FCRLA	4.1	HLA-DRB1	-11.7	MT1X	3.1	SRGN	-3.1
SQLE	4	HLA-DMB	-11.1	COL16A1	3	NPTX1	-2.8
PRUNE2	4	HLA-DPA1	-10.4	MAL	2.8	PENK	-2.7
SLC2A10	3.8	ARHGDIB	-9.7	BMF	2.7	CAPS	-2.4
SNAI2	3.5	TYROBP	-8.7	SSX5	2.7	ODC1	-2.3
FADS1	2.9	SLC15A3	-6.4	MT1G	2.5	RNU1A3	-2.3
ECH1	2.7	HBA2	-6.3	AEBP1	2.5	CYR61	-2.3
PLIN2	2.5	HBB	-5.5	CDH19	2.4	LOC389342	-2.3
DHCR7	2.5	ITGB2	-5.2	CLCNKA	2.4	MAL2	-2.1
OSBPL9	2.5	IL18BP	-4.9	PKNOX2	2.4	CDCA7	-2.1
BMF	2.5	SNORD3A	-4.5	PDK4	2.2	WFDC1	-2.1
PDK4	2.5	CD68	-3.7	MT2A	2.2	HSP90B1	-2.2
LSS	2.4	CXCL16	-3.5	SLC2A10	2.2	IFI6	-2.2
MT2A	2.4	CD8A	-3.3	GPR125	2.2	LAMA1	-2.2
SC4MOL	2.3	CD3D	-2.7	LSS	2.1	THBS2	-2.2
PECI	2.1	CDH1	-2.6	CREB1	2.1	CTSL1	-2.2
MT1E	2.1	VCAM1	-2.1	MT1E	2.1	EIF5A	-2
ACOT1	2	CD2	-2.1	FADS1	2	QPCT	-2

intracellular lipolysis, thus supplying substrate for fatty acid oxidation (FAO) [35]. Upregulation of FAO in MCTS is indicated by upregulation of *enoyl-CoA hydratase 1* (*ECH1*; Gene ID: 1891, OMIM 600696), *peroxisomal D3,D2-enoyl-CoA isomerase* (*PECI;* Gene ID: 10455, OMIM 608024), and *acyl-CoA thioesterase 1 (ACOT1*, Gene ID: 641371, OMIM 614313; Table 1). FAO has been proven to be an advantageous metabolic trait for cancer cells and is linked to anoikis resistance [36].

MCTS culture conditions induce a metabolic shift toward a lipogenic profile: Microarray results indicated a metabolic shift toward a lipogenic profile in the MCTS. A high content of lipid droplets (LDs) and stored-cholesterol ester is strongly associated with tumor aggressiveness [37,38]. As shown in Table 1, *ACOT1* (lipid metabolism), *fatty acid desaturase 1* (*FADS1*, Gene ID: 3992, OMIM 606148; biosynthesis of unsaturated fatty acids), *sterol-C4-mehtyl oxidase-like* (*SC4MOL,* Gene ID: 6307, OMIM 607545), *7-dehydrocholesterol reductase* (*DHCR7,* Gene ID: 1717, OMIM 602858), *lanosterol synthase* (*LSS*, Gene ID: 4047, OMIM 600909; cholesterol biosynthesis), and *oxysterol binding protein like 9* (*OSBPL9,* Gene ID: 114883, OMIM 606737; intracellular lipid receptor) all showed marked upregulation in the MCTS cultures compared to primary tumors. *SC4MOL, LSS*, and *FAD1* were also found to be upregulated in the MCTS cultures compared to the adherent cultures. The microarray results also demonstrated increased lipid storage by upregulation of *perilipin 2* (*PLIN2,* Gene ID: 123, OMIM 103195). *PLIN2* belongs to the perilipin family, members of which

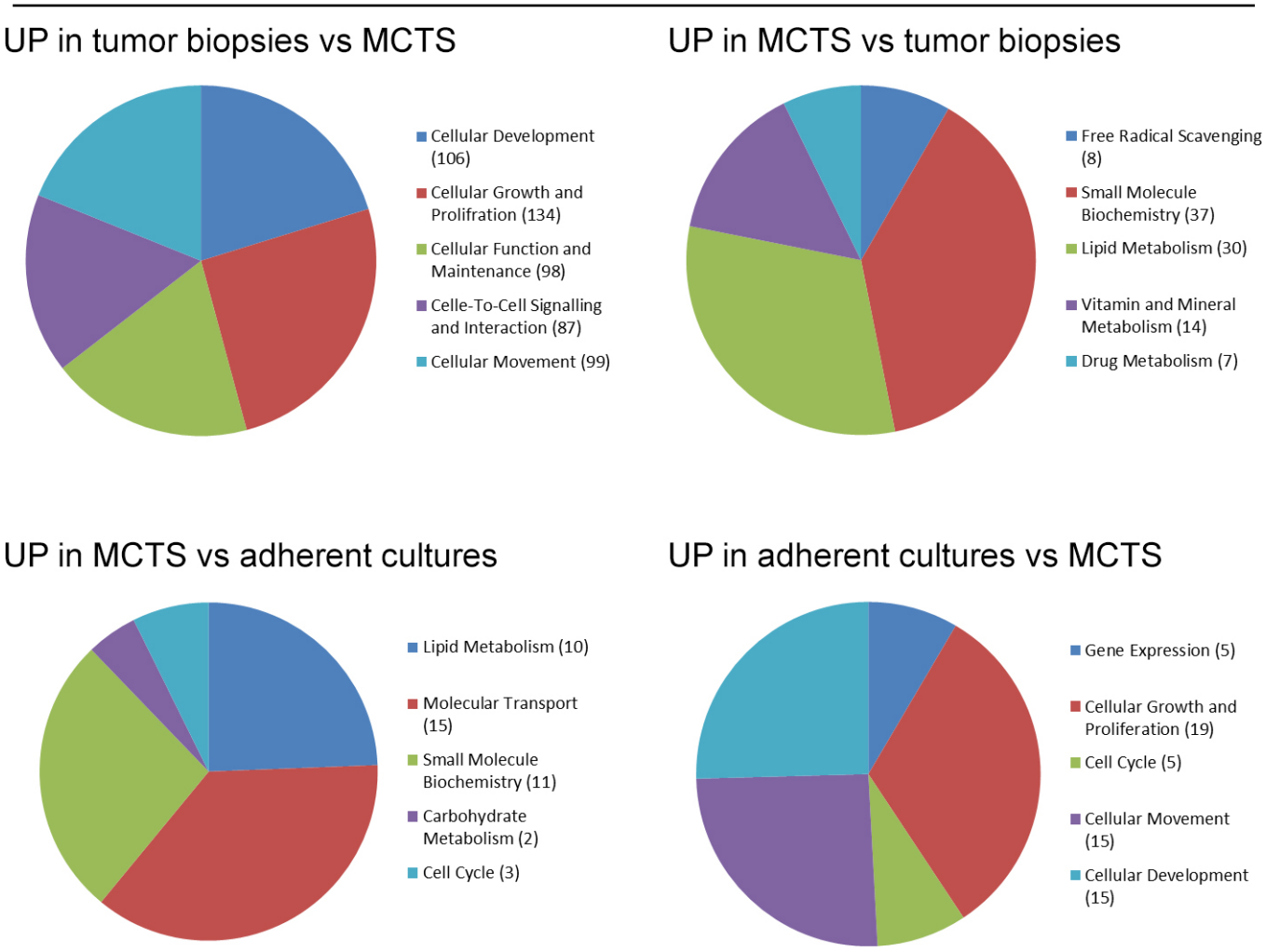

Figure 3. Molecular and cellular functions being upregulated in tumor biopsies versus multicellular tumor spheroids (upper left panel), multicellular tumor spheroids versus tumor biopsies (upper right panel), multicellular tumor spheroids versus adherent cultures (lower left panel), and adherent cultures versus multicellular tumor spheroids (lower right panel). The number of molecules upregulated is shown in brackets. MCTS = tumors cultivated as multicellular tumor spheroids; adherent cultures = adherent cultivated tumors; tumor biopsies = uncultured primary tumor tissue.

coat intracellular lipid storage droplets [39]. The presence of PLIN2 was verified with IHC of donors D1, D2, and D3 (Figure 4). Morphological examination with transmission electron microscopy (TEM) revealed numerous lipid droplets in the supplementary donor D(S) cultured as MCTS (Figure 5). The TEM images also showed numerous mitochondria.

MCTS cultures increase the expression of cancer and testis antigens: The *synovial sarcoma X breakpoint* (*SSX,* Gene ID: 6759, OMIM 300326) gene family consists of nine highly homologous members (*SSX1–9*) [40]. *SSX* expression is confined to the testis, placenta, at low levels in the thyroid, and in a wide range of tumors (including synovial sarcoma), thus making them interesting targets for cancer therapy [41]. SSXs have been linked to EMT and anoikis resistance [42].

The microarray results showed an increase in the expression of *SSX4* in MCTS versus primary tumors and adherent cultures (Table 1). This presence of *SSX4* mRNA was verified with RNAscope, while the SSX4 protein was verified with IHC staining. The proportion of cells expressing SSX4 in primary tumors and MCTS was found (Figure 6). Noticeably, the SSX protein was minimally expressed in the tumor biopsies.

DISCUSSION

By comparing the UM MCTS to biopsies and adherent cell cultures, the present study revealed a metabolic shift in the MCTS. The latter display traits associated with anoikis resistance, including a shift toward a lipogenic profile, as well as marked upregulation of SSXs, transcriptional repressors capable of humoral and cellular immune responses in cancer patients and putative targets for immunotherapy in cancers.

To disseminate, cancer cells have to undergo loss of adherence. Loss of adherence inhibits uptake of glucose and glycolysis which results in diminished levels of ATP and NADPH leading to metabolic stress and generation of ROS that induces anoikis [15]. The induction of FAO restores ATP production and increases NADPH, thus preventing anoikis [15,43]. This metabolic shift is also indicated in the MCTS

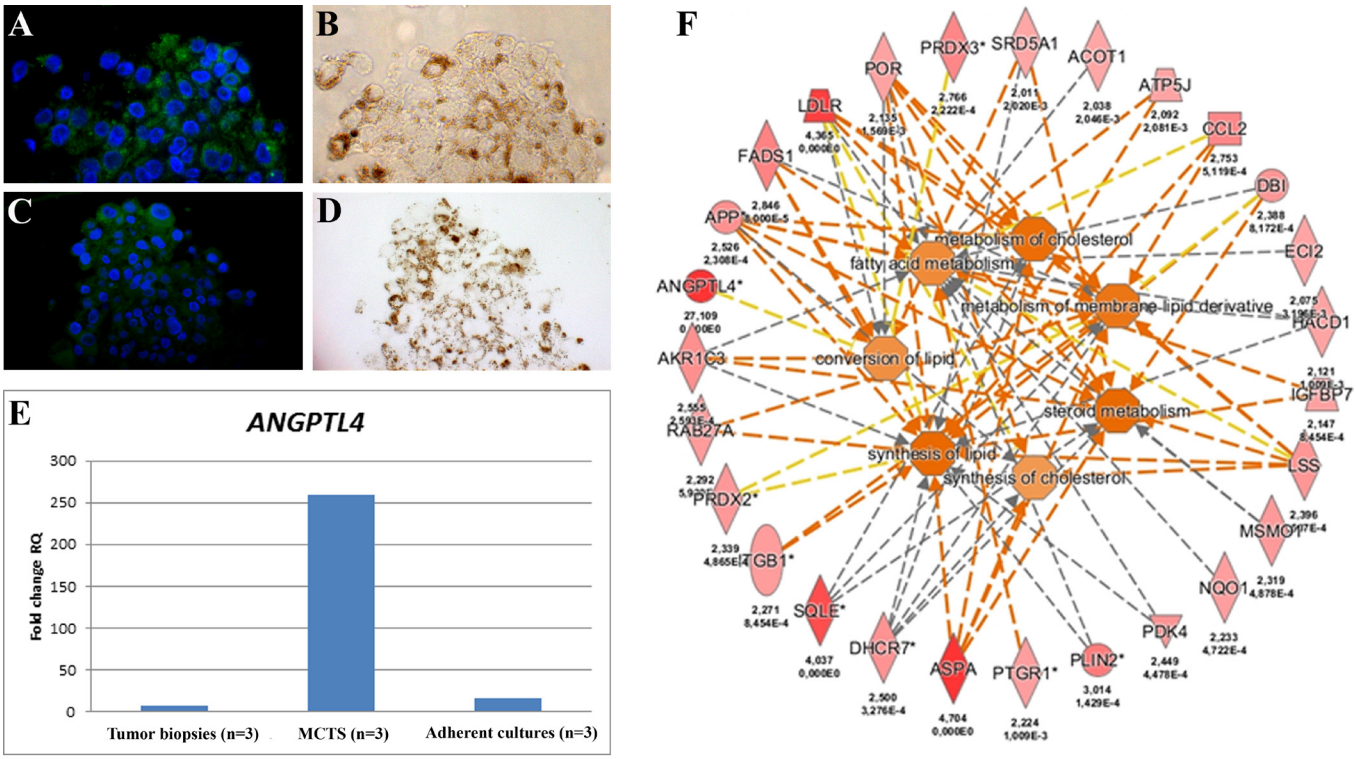

Figure 4. Lipogenic profile of uveal melanoma multicellular tumor spheroids. Angiopoietin like 4 (*ANGPTL4*; green) staining of multicellular tumor spheroids (MCTS), Hoechst staining of nucleus (blue; **A**) with corresponding light-microscopic image (**B**). Perilipin 2 (PLIN2) staining (green) of MCTS and Hoechst staining of the nucleus (blue; **C**) with the corresponding light microscopic image (**D**). **E**: Quantitative reverse-transcription PCR (qRT-PCR) of *ANGPTL4* in support of the microarray finding. **F**: Ingenuity Pathway Analysis (IPA) based on rank product ($q \leq 0.05$) in MCTS versus the tumor, showing important molecules and pathways, including seven networks and their associated upregulated molecules in lipid metabolism. Deep red indicates more pronounced expression, and numbers below the gene symbols reflect the fold change (number on top) and q value/significance (number below).

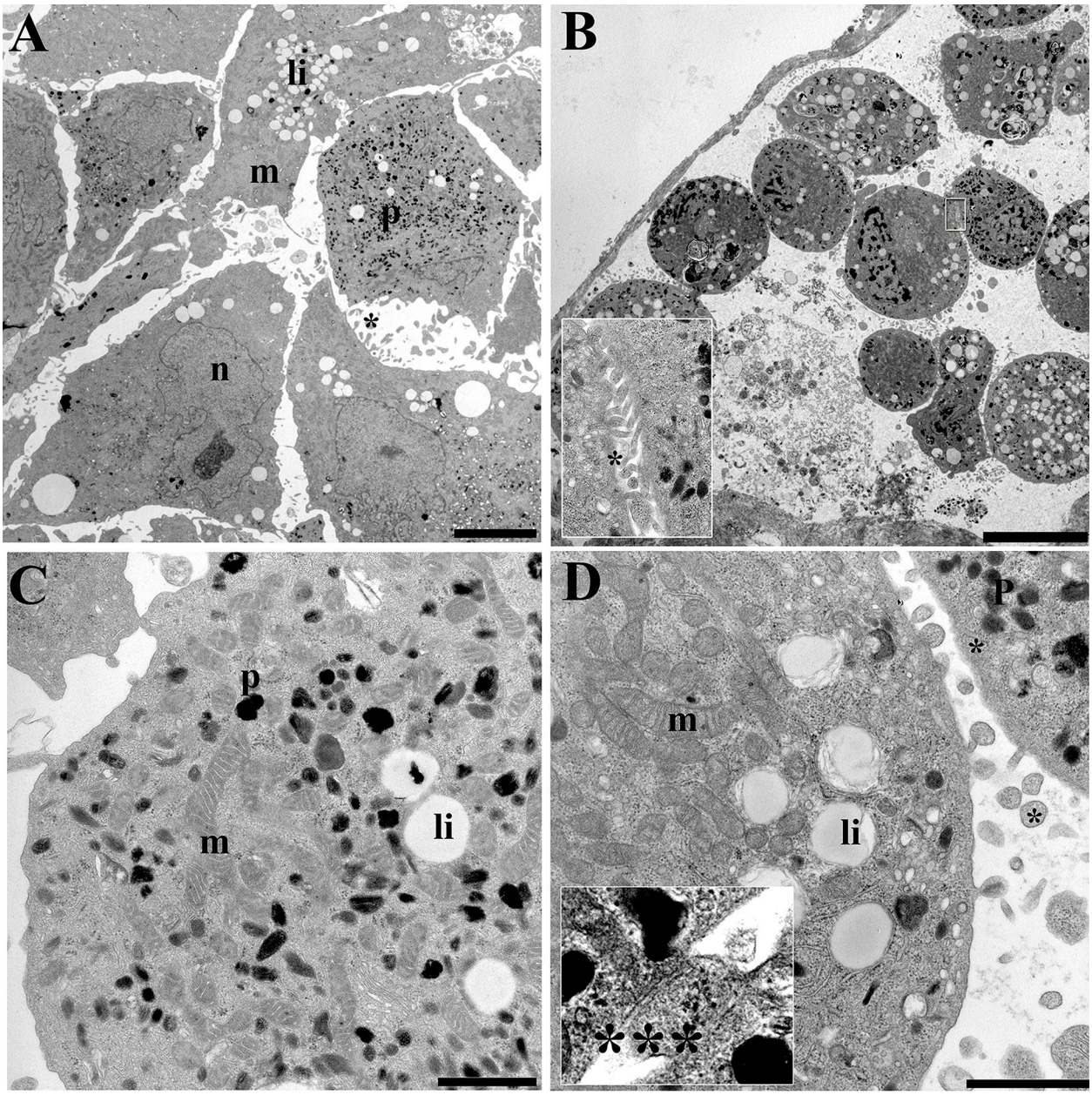

Figure 5. Transmission electron microscopy of uveal melanoma. **A**: Uveal melanoma biopsy with nucleus (n), lipid droplets (li), pigment (p), mitocondria (m) and interdigitations (*) between cells. **B**–**D**: In the multicellular tumor spheroids (MCTS), the cells were less packed but contained abundant lipid droplets, pigment, interdigitations, and a dense concentration of mitochondria. **D**: Adherence-like junctions (***) between cells were also evident (inset). Scale bars: **A**, 5 µm; **B**, 10 µm; **C**, 1 µm; **D**, 1 µm.

in the present study. Malignant cells have been shown to provide and utilize fatty acids [36]. The lipogenic profile of the MCTS-derived cells reveals an increase in the synthesis of cholesterol, a trait associated with cancer aggressiveness [38,44,45]. Depletion of cholesterol has been shown to result in anoikis-like cell death [46]. Whether the lipogenic switch seen in the MCTS in the present study is valid for in vivo disseminated UM cells remains to be revealed. Lipogenic targeting could be advantageous for solid tumors. The present study showed abundant LDs in the MCTS and in the primary tumor. The presence of LDs in UM has been described in the literature previously, as a response to radiation and in the untreated tumor tissue [47,48]. UM is characterized by its poor response to chemotherapeutics, and FAO has been shown to fuel chemoresistant cancer cells [49]. Several FAO inhibitors have shown promising results in mice models, although

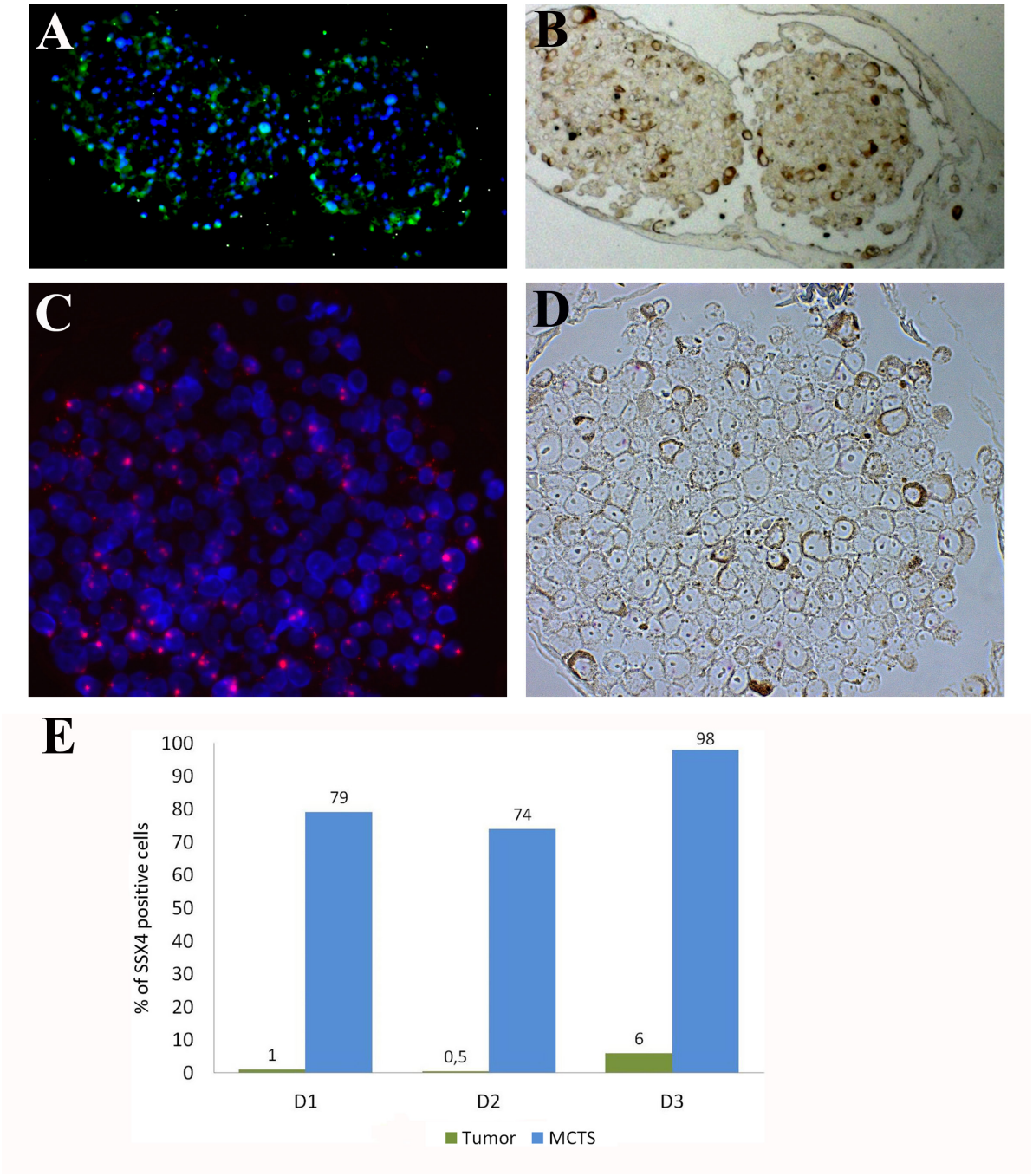

Figure 6. Immunohistochemistry analysis of uveal melanoma multicellular tumor spheroids shows positive staining for SSX4 (green), Hoechst staining of nucleus (blue; **A**) with corresponding light-microscopic image (**B**). The presence of synovial sarcoma X breakpoint protein 4 (SSX4) was verified with RNAscope staining (red), Hoechst staining of nucleus (blue; **C**) where *SSX4* RNA transcripts are shown as red chromogenic dots, and with the corresponding light-microscopic image (**D**). **E**: Percentage of SSX4-positive cells in multicellular tumor spheroids (MCTS) (D1, D2, and D3) versus uncultured primary tumors (D1, D2, and D3) analyzed with immunohistochemistry (IHC).

chemosensitization by FAO and cholesterol synthesis inhibitors might be even more favorable [50-52]. The present results imply that *ANGPTL4* might be a key player in orchestrating lipid metabolism in MCTS. *ANGPTL4* has previously been shown to play a role in anoikis resistance and in angiogenesis and oncogenesis of several cancers, including UM [34,53-55]. The link between *ANGPTL4* and EMT has recently been highlighted as a decrease in EMT markers and aggressiveness after silencing of ANGPTL4 in non-small cell lung cancer [56]. Although most publications indicate an oncogenic function of *ANGPTL4*, the opposite has been shown in gastric cancer, where it is a proposed tumor suppressor [57]. These conflicting findings suggest that further characterization of *ANGPTL4* in UM is needed. The present results suggest that ANGPTL4 could be an attractive target in UM and possibly a way to target disseminated cancer cells.

Another compelling finding in the present study is the marked upregulation of *SSX4*. *SSX*s show tissue-restricted expression and are therefore regarded as attractive targets for cancer therapy [40,58]. The proteins are implied to be involved in proliferation and survival in cancer cells and formed a transient complex with beta-catenin thus altering the expression of genes involved in EMT [59]. SSXs are localized to the nucleus and contains two different repressor domains: a Krüppel associated box (KRAB) domain and a potent repressor domain (RD) [60,61]. SSXs have a close connection with the Polycomb repressive group of proteins [62,63]. *SSX2* (a homologous SSX group member) has been shown to antagonize BMI1 and EZH2 through an indirect mechanism, thus activating repressed genes. Additionally, SSX2 has been shown to have DNA-binding properties and negatively regulate the distribution of histone mark H3K27me3, implying that SSX2 plays a role in the regulation of chromatin structure and function [64]. The exact function of SSXs in UM is not known, although the link between EMT and SSXs highlights a potential role in anoikis resistance. Disseminated cancer cells are likely to have an altered metabolic state as a survival strategy, and *SSX*s with their gene-regulating properties might be essential for these alterations. The synovial sarcoma fusion protein SS18-SSX2 has been associated with induction of cholesterol synthesis [65]. Whether there is a direct link between lipid metabolism and SSXs in UM is yet to be unveiled. SSX4 has been shown to be expressed in 21% of skin melanomas; however, *SSX4* expression in UM has not yet been assessed [41]. If SSXs are highly expressed in disseminated cancer cells, it would make them valuable targets for immunotherapy. The restricted tissue expression of SSXs might lead to less severe side effects than targeting molecules and pathways involved in normal cellular homeostasis.

Cell culturing of UM is often hampered by tumor size and growth properties. A limitation of the present study is the low number and histological homogeneity of the donors included. In our experience, spindle cell tumors are more challenging to cultivate, thus making it difficult to run extensive genomic analyses on this cell type. Tumor size is an important aspect in UM research as the relative size of the tumors is small compared to other cancers, such as colon and breast. The diagnostic assessment should always be prioritized, meaning that miniscule amounts of tissue are available for research if the primary tumor is small. Unfortunately, small tissue samples (as often seen in spindle cell UM) also show greater clonal homogeneity upon expansion provided that the same number of cells is needed for downstream analyses. By using samples from larger tumors and early cell culture passages, we hope to better reflect the innate properties of the primary tumor. Epitheloid and mixed tumors are more prone to metastasis. The donors D1, D2, and D3 all had confirmed liver metastases. The selection of tumors analyzed in this study therefore is highly representative of aggressive UMs. Whether these results are valid for all UMs or solely the aggressive UMs is yet to be revealed, although there are indications that tumors with a low metastatic risk profile are more difficult to cultivate using the present protocol. The optimization of culture conditions would enable us to conduct further experiments for extensive verification of results and unravelling of epigenetic pathways.

In conclusion, we found that UM MCTS cultures undergo a metabolic shift. The MCTS display traits associated with anoikis resistance, including a shift toward a lipogenic profile. Targeting of lipid metabolism as a method to kill disseminated cancer cells could be a compelling new therapy in UM and needs further investigation. Additionally, the present study showed marked upregulation of SSXs, transcriptional repressors related to the PcG proteins that modulate epigenetic silencing of genes. SSXs have been implied in the process of EMT, and their expression could be increased in cells that have conferred anoikis resistance, thus serving as a potential target for disseminated cancer cells. UM MCTS could be a suitable model to reveal novel candidate targets for treatment of UM dissemination.

APPENDIX 1. J-EXPRESS AND RANK PRODUCT (RP) ANALYSIS OF DIFFERENTIALLY EXPRESSED GENES (≥2 FOLD UP/DOWN, Q≤ 0.05) IN MULTICELLULAR TUMOR SPHEROIDS (MCTS) VERSUS UNCULTURED TUMOR BIOPSIES VS ADHERENT PRIMARY CULTURES.

To access the data, click or select the words "Appendix 1."

ACKNOWLEDGMENTS

We would like to acknowledge all personnel at the Center for Eye Research and at the Dep. of Ophthalmology OUS that contributed in this project. We thank the personnel at the Genomics Core Facility, OUS and Helse Sør-Øst for performing microarray analysis and helping out with J-express analysis. We would also like to thank Sverre-Henning Brorson at the Dep. of Pathology, OUS for helping with TEM imaging. The work was funded by the South-Eastern Norway Regional Health Authority (Helse Sør-Øst) project 2012104, Norwegian Cancer Society project 5808589 and supported by grants from Arthur and Odd Clausons ophthalmological fund, Aase and Knut Tønjums ophthalmological fund, Futura fund, Unifor Frimed, Norwegian Association of the Blind and Partially Sighted, Inger Holms memorial fund, Stiftelsen for fremme av kreftforskning at University of Oslo and Legat til fremme av kreftforskning. All authors contributing to the study have read and approved the manuscript. There are no conflicts of interest for any of the authors.

REFERENCES

1. Singh AD, Turell ME, Topham AK. Uveal Melanoma: Trends in Incidence, Treatment, and Survival. Ophthalmology 2011; 118:1881-5. [PMID: 21704381].

2. Virgili G, Gatta G, Ciccolallo L, Capocaccia R, Biggeri A, Crocetti E, Lutz JM, Paci E. Incidence of uveal melanoma in Europe. Ophthalmology 2007; 114:2309-15. [PMID: 17498805].

3. Bergman L, Seregard S, Nilsson B, Lundell G, Ringborg U, Ragnarsson-Olding B. Uveal melanoma survival in Sweden from 1960 to 1998. Invest Ophthalmol Vis Sci 2003; 44:3282-7. [PMID: 12882771].

4. Kujala E, Makitie T, Kivela T. Very long-term prognosis of patients with malignant uveal melanoma. Invest Ophthalmol Vis Sci 2003; 44:4651-9. [PMID: 14578381].

5. Diener-West M, Reynolds SM, Agugliaro DJ, Caldwell R, Cumming K, Earle JD, Hawkins BS, Hayman JA, Jaiyesimi I, Jampol LM, Kirkwood JM, Koh WJ, Robertson DM, Shaw JM, Straatsma BR, Thoma J. Development of metastatic disease after enrollment in the COMS trials for treatment of choroidal melanoma: Collaborative Ocular Melanoma Study Group Report No. 26. Arch Ophthalmol 2005; 123(12):1639–43.

6. Tura A, Luke J, Merz H, Reinsberg M, Luke M, Jager MJ, Grisanti S. Identification of circulating melanoma cells in uveal melanoma patients by dual-marker immunoenrichment. Invest Ophthalmol Vis Sci 2014; 55:4395-404. [PMID: 24970258].

7. Kaliki S, Shields CL, Shields JA. Uveal melanoma: Estimating prognosis. Indian J Ophthalmol 2015; 63:93-102. [PMID: 25827538].

8. Callejo SA, Antecka E, Blanco PL, Edelstein C, Burnier MN Jr. Identification of circulating malignant cells and its correlation with prognostic factors and treatment in uveal melanoma. A prospective longitudinal study. Eye (Lond) 2007; 21:752-9. [PMID: 16575415].

9. Eide N, Faye RS, Hoifodt HK, Overgaard R, Jebsen P, Kvalheim G, Fodstad O. Immunomagnetic detection of micrometastatic cells in bone marrow in uveal melanoma patients. Acta ophthalmologica 2009; 87:830-6. [PMID: 19055657].

10. Eide N, Faye RS, Hoifodt HK, Sandstad B, Qvale G, Faber R, Jebsen P, Kvalheim G, Fodstad O. Immunomagnetic detection of micrometastatic cells in bone marrow of uveal melanoma patients: a paradox. Acta ophthalmologica 2015; 93:59-66. [PMID: 25613126].

11. Sullivan WJ, Christofk HR. The metabolic milieu of metastases. Cell 2015; 160:363-4. [PMID: 25635452].

12. Nguyen DX, Bos PD, Massague J. Metastasis: from dissemination to organ-specific colonization. Nat Rev Cancer 2009; 9:274-84. [PMID: 19308067].

13. Kondo T. Stem cell-like cancer cells in cancer cell lines. Cancer biomarkers: section Dis Markers 2007; 3:245-50. .

14. Buchheit CL, Weigel KJ, Schafer ZT. Cancer cell survival during detachment from the ECM: multiple barriers to tumour progression. Nat Rev Cancer 2014; 14:632-41. [PMID: 25098270].

15. Schafer ZT, Grassian AR, Song L, Jiang Z, Gerhart-Hines Z, Irie HY, Gao S, Puigserver P, Brugge JS. Antioxidant and oncogene rescue of metabolic defects caused by loss of matrix attachment. Nature 2009; 461:109-13. [PMID: 19693011].

16. Paoli P, Giannoni E, Chiarugi P. Anoikis molecular pathways and its role in cancer progression. Biochim Biophys Acta 2013; 1833:3481-98. [PMID: 23830918].

17. Weiswald LB, Richon S, Validire P, Briffod M, Lai-Kuen R, Cordelieres FP, Bertrand F, Dargere D, Massonnet G, Marangoni E, Gayet B, Pocard M, Bieche I, Poupon MF, Bellet D, Dangles-Marie V. Newly characterised ex vivo colospheres as a three-dimensional colon cancer cell model of tumour aggressiveness. Br J Cancer 2009; 101:473-82. [PMID: 19603013].

18. Emmink BL, Van Houdt WJ, Vries RG, Hoogwater FJ, Govaert KM, Verheem A, Nijkamp MW, Steller EJ, Jimenez CR, Clevers H, Borel Rinkes IH, Kranenburg O. Differentiated human colorectal cancer cells protect tumor-initiating cells from irinotecan. Gastroenterology 2011; 141:269-78. [PMID: 21459094].

19. Calvet CY, Andre FM, Mir LM. The culture of cancer cell lines as tumorspheres does not systematically result in cancer stem cell enrichment. PLoS One 2014; 9:e89644-[PMID: 24586931].

20. Kunjithapatham R, Karthikeyan S, Geschwind JF, Kieserman E, Lin M, Fu DX, Ganapathy-Kanniappan S. Reversal of

anchorage-independent multicellular spheroid into a monolayer mimics a metastatic model. Sci Rep 2014; 4:6816-[PMID: 25351825].

21. Weiswald LB, Bellet D, Dangles-Marie V. Spherical cancer models in tumor biology. Neoplasia 2015; 17:1-15. [PMID: 25622895].

22. Nareyeck G, Zeschnigk M, Bornfeld N, Anastassiou G. Novel cell lines derived by long-term culture of primary uveal melanomas. Ophthalmologica Journal international d'ophtalmologie International journal of ophthalmology Z Augenheilkd 2009; 223:196-201. .

23. Fang D, Nguyen TK, Leishear K, Finko R, Kulp AN, Hotz S, Van Belle PA, Xu X, Elder DE, Herlyn M. A tumorigenic subpopulation with stem cell properties in melanomas. Cancer Res 2005; 65:9328-37. [PMID: 16230395].

24. Schroeder A, Mueller O, Stocker S, Salowsky R, Leiber M, Gassmann M, Lightfoot S, Menzel W, Granzow M, Ragg T. The RIN: an RNA integrity number for assigning integrity values to RNA measurements. BMC Mol Biol 2006; 7:3-[PMID: 16448564].

25. Johnsen EO, Froen RC, Albert R, Omdal BK, Sarang Z, Berta A, Nicolaissen B, Petrovski G, Moe MC. Activation of neural progenitor cells in human eyes with proliferative vitreoretinopathy. Exp Eye Res 2012; 98:28-36. [PMID: 22465407].

26. Breitling R, Armengaud P, Amtmann A, Herzyk P. Rank products: a simple, yet powerful, new method to detect differentially regulated genes in replicated microarray experiments. FEBS Lett 2004; 573:83-92. [PMID: 15327980].

27. Wang F, Flanagan J, Su N, Wang LC, Bui S, Nielson A, Wu X, Vo HT, Ma XJ, Luo Y. RNAscope: a novel in situ RNA analysis platform for formalin-fixed, paraffin-embedded tissues. JMD 2012; 14:22-9. [PMID: 22166544].

28. Murdoch A, Jenkinson EJ, Johnson GD, Owen JJ. Alkaline phosphatase-fast red, a new fluorescent label. Application in double labelling for cell cycle analysis. J Immunol Methods 1990; 132:45-9. [PMID: 2118160].

29. van Essen TH, van Pelt SI, Bronkhorst IH, Versluis M, Nemati F, Laurent C, Luyten GP, van Hall T, van den Elsen PJ, van der Velden PA, Decaudin D, Jager MJ. Upregulation of HLA Expression in Primary Uveal Melanoma by Infiltrating Leukocytes. PLoS One 2016; 11:e0164292-[PMID: 27764126].

30. Frisch SM, Francis H. Disruption of epithelial cell-matrix interactions induces apoptosis. J Cell Biol 1994; 124:619-26. [PMID: 8106557].

31. Onder TT, Gupta PB, Mani SA, Yang J, Lander ES, Weinberg RA. Loss of E-cadherin promotes metastasis via multiple downstream transcriptional pathways. Cancer Res 2008; 68:3645-54. [PMID: 18483246].

32. Kamarajugadda S, Stemboroski L, Cai Q, Simpson NE, Nayak S, Tan M, Lu J. Glucose oxidation modulates anoikis and tumor metastasis. Mol Cell Biol 2012; 32:1893-907. [PMID: 22431524].

33. Hu K, Babapoor-Farrokhran S, Rodrigues M, Deshpande M, Puchner B, Kashiwabuchi F, Hassan SJ, Asnaghi L, Handa JT, Merbs S, Eberhart CG, Semenza GL, Montaner S, Sodhi A. Hypoxia-inducible factor 1 upregulation of both VEGF and ANGPTL4 is required to promote the angiogenic phenotype in uveal melanoma. Oncotarget 2016; [PMID: 26761211].

34. Zhang Z, Cao L, Li J, Liang X, Liu Y, Liu H, Du J, Qu Z, Cui M, Liu S, Gao L, Ma C, Zhang L, Han L, Sun W. Acquisition of anoikis resistance reveals a synoikis-like survival style in BEL7402 hepatoma cells. Cancer Lett 2008; 267:106-15. [PMID: 18433990].

35. Gray NE, Lam LN, Yang K, Zhou AY, Koliwad S, Wang JC. Angiopoietin-like 4 (Angptl4) protein is a physiological mediator of intracellular lipolysis in murine adipocytes. J Biol Chem 2012; 287:8444-56. [PMID: 22267746].

36. Carracedo A, Cantley LC, Pandolfi PP. Cancer metabolism: fatty acid oxidation in the limelight. Nat Rev Cancer 2013; 13:227-32. [PMID: 23446547].

37. Yue S, Li J, Lee SY, Lee HJ, Shao T, Song B, Cheng L, Masterson TA, Liu X, Ratliff TL, Cheng JX. Cholesteryl ester accumulation induced by PTEN loss and PI3K/AKT activation underlies human prostate cancer aggressiveness. Cell Metab 2014; 19:393-406. [PMID: 24606897].

38. Beloribi-Djefaflia S, Vasseur S, Guillaumond F. Lipid metabolic reprogramming in cancer cells. Oncogenesis 2016; 5:e189-[PMID: 26807644].

39. Kimmel AR, Brasaemle DL, McAndrews-Hill M, Sztalryd C, Londos C. Adoption of PERILIPIN as a unifying nomenclature for the mammalian PAT-family of intracellular lipid storage droplet proteins. J Lipid Res 2010; 51:468-71. [PMID: 19638644].

40. Smith HA, McNeel DG. The SSX family of cancer-testis antigens as target proteins for tumor therapy. Clin Dev Immunol 2010; 2010:150591-[PMID: 20981248].

41. Tureci O, Chen YT, Sahin U, Gure AO, Zwick C, Villena C, Tsang S, Seitz G, Old LJ, Pfreundschuh M. Expression of SSX genes in human tumors. Int J Cancer 1998; 77:19-23. [PMID: 9639388].

42. Frisch SM, Schaller M, Cieply B. Mechanisms that link the oncogenic epithelial-mesenchymal transition to suppression of anoikis. J Cell Sci 2013; 126:21-9. [PMID: 23516327].

43. Pike LS, Smift AL, Croteau NJ, Ferrick DA, Wu M. Inhibition of fatty acid oxidation by etomoxir impairs NADPH production and increases reactive oxygen species resulting in ATP depletion and cell death in human glioblastoma cells. Biochim Biophys Acta 2011; 1807:726-34. [PMID: 21692241].

44. Kuzu OF, Noory MA, Robertson GP. The Role of Cholesterol in Cancer. Cancer Res 2016; 76:2063-70. [PMID: 27197250].

45. Mollinedo F, Gajate C. Lipid rafts as major platforms for signaling regulation in cancer. Adv Biol Regul 2015; 57:130-46. [PMID: 25465296].

46. Park EK, Park MJ, Lee SH, Li YC, Kim J, Lee JS, Lee JW, Ye SK, Park JW, Kim CW, Park BK, Kim YN. Cholesterol depletion induces anoikis-like apoptosis via FAK down-regulation and caveolae internalization. J Pathol 2009; 218:337-49. [PMID: 19288501].

47. Seddon JM, Gragoudas ES, Albert DM. Ciliary body and choroidal melanomas treated by proton beam irradiation. Histopathologic study of eyes. Arch Ophthalmol 1983; 101:1402-8. [PMID: 6311146].

48. Driot JY, Rault J, Bonnin P, Liotet S. Electron microscopy of three cases of choroid malignant melanomas. Int Ophthalmol 1987; 10:193-202. [PMID: 3654058].

49. Harper ME, Antoniou A, Villalobos-Menuey E, Russo A, Trauger R, Vendemelio M, George A, Bartholomew R, Carlo D, Shaikh A, Kupperman J, Newell EW, Bespalov IA, Wallace SS, Liu Y, Rogers JR, Gibbs GL, Leahy JL, Camley RE, Melamede R, Newell MK. Characterization of a novel metabolic strategy used by drug-resistant tumor cells. FASEB J 2002; 16:1550-7. [PMID: 12374777].

50. Schlaepfer IR, Rider L, Rodrigues LU, Gijon MA, Pac CT, Romero L, Cimic A, Sirintrapun SJ, Glode LM, Eckel RH, Cramer SD. Lipid catabolism via CPT1 as a therapeutic target for prostate cancer. Mol Cancer Ther 2014; 13:2361-71. [PMID: 25122071].

51. Hossain F, Al-Khami AA, Wyczechowska D, Hernandez C, Zheng L, Reiss K, Valle LD, Trillo-Tinoco J, Maj T, Zou W, Rodriguez PC, Ochoa AC. Inhibition of Fatty Acid Oxidation Modulates Immunosuppressive Functions of Myeloid-Derived Suppressor Cells and Enhances Cancer Therapies. Cancer Immunol Res 2015; 3:1236-47. [PMID: 26025381].

52. Kodach LL, Jacobs RJ, Voorneveld PW, Wildenberg ME, Verspaget HW, van Wezel T, Morreau H, Hommes DW, Peppelenbosch MP, van den Brink GR, Hardwick JC. Statins augment the chemosensitivity of colorectal cancer cells inducing epigenetic reprogramming and reducing colorectal cancer cell 'stemness' via the bone morphogenetic protein pathway. Gut 2011; 60:1544-53. [PMID: 21551187].

53. Tan MJ, Teo Z, Sng MK, Zhu P, Tan NS. Emerging roles of angiopoietin-like 4 in human cancer. Molecular cancer research MCR. 2012; 10:677-88. [PMID: 22661548].

54. Zhu P, Tan MJ, Huang RL, Tan CK, Chong HC, Pal M, Lam CR, Boukamp P, Pan JY, Tan SH, Kersten S, Li HY, Ding JL, Tan NS. Angiopoietin-like 4 protein elevates the prosurvival intracellular O2(-):H2O2 ratio and confers anoikis resistance to tumors. Cancer Cell 2011; 19:401-15. [PMID: 21397862].

55. Tanaka J, Irie T, Yamamoto G, Yasuhara R, Isobe T, Hokazono C, Tachikawa T, Kohno Y, Mishima K. ANGPTL4 regulates the metastatic potential of oral squamous cell carcinoma. J Oral Pathol Med 2015; 44:126-33. [PMID: 25060575].

56. Zhu X, Guo X, Wu S, Wei L. ANGPTL4 Correlates with NSCLC Progression and Regulates Epithelial-Mesenchymal Transition via ERK Pathway. Lung 2016; [PMID: 27166634].

57. Okochi-Takada E, Hattori N, Tsukamoto T, Miyamoto K, Ando T, Ito S, Yamamura Y, Wakabayashi M, Nobeyama Y, Ushijima T. ANGPTL4 is a secreted tumor suppressor that inhibits angiogenesis. Oncogene 2014; 33:2273-8. [PMID: 23686315].

58. Abate-Daga D, Speiser DE, Chinnasamy N, Zheng Z, Xu H, Feldman SA, Rosenberg SA, Morgan RA. Development of a T cell receptor targeting an HLA-A*0201 restricted epitope from the cancer-testis antigen SSX2 for adoptive immunotherapy of cancer. PLoS One 2014; 9:e93321-[PMID: 24681846].

59. D'Arcy P, Maruwge W, Wolahan B, Ma L, Brodin B. Oncogenic functions of the cancer-testis antigen SSX on the proliferation, survival, and signaling pathways of cancer cells. PLoS One 2014; 9:e95136-[PMID: 24787708].

60. dos Santos NR, de Bruijn DR, Balemans M, Janssen B, Gartner F, Lopes JM, de Leeuw B, Geurts van Kessel A. Nuclear localization of SYT, SSX and the synovial sarcoma-associated SYT-SSX fusion proteins. Hum Mol Genet 1997; 6:1549-58. [PMID: 9285793].

61. Lim FL, Soulez M, Koczan D, Thiesen HJ, Knight JC. A KRAB-related domain and a novel transcription repression domain in proteins encoded by SSX genes that are disrupted in human sarcomas. Oncogene 1998; 17:2013-8. [PMID: 9788446].

62. Kato H, Tjernberg A, Zhang W, Krutchinsky AN, An W, Takeuchi T, Ohtsuki Y, Sugano S, de Bruijn DR, Chait BT, Roeder RG. SYT associates with human SNF/SWI complexes and the C-terminal region of its fusion partner SSX1 targets histones. J Biol Chem 2002; 277:5498-505. [PMID: 11734557].

63. Soulez M, Saurin AJ, Freemont PS, Knight JC. SSX and the synovial-sarcoma-specific chimaeric protein SYT-SSX co-localize with the human Polycomb group complex. Oncogene 1999; 18:2739-46. [PMID: 10348348].

64. Gjerstorff MF, Relster MM, Greve KB, Moeller JB, Elias D, Lindgreen JN, Schmidt S, Mollenhauer J, Voldborg B, Pedersen CB, Bruckmann NH, Mollegaard NE, Ditzel HJ. SSX2 is a novel DNA-binding protein that antagonizes polycomb group body formation and gene repression. Nucleic Acids Res 2014; 42:11433-46. [PMID: 25249625].

65. de Bruijn DR, Allander SV, van Dijk AH, Willemse MP, Thijssen J, van Groningen JJ, Meltzer PS, van Kessel AG. The synovial-sarcoma-associated SS18–SSX2 fusion protein induces epigenetic gene (de)regulation. Cancer Res 2006; 66:9474-82. [PMID: 17018603].

Articles are provided courtesy of Emory University and the Zhongshan Ophthalmic Center, Sun Yat-sen University, P.R. China. The print version of this article was created on 3 October 2017. This reflects all typographical corrections and errata to the article through that date. Details of any changes may be found in the online version of the article.